Mechanical Design of RF MEMS Capacitive Switches

J. De Coster, H.A.C. Tilmans[*], K. Hameyer, R. Puers

Katholieke Universiteit Leuven
Electrical Engineering Department – ESAT, Division MICAS – ELECTA
Kasteelpark Arenberg 10, 3001 Heverlee, Belgium
Phone: +32 (0)16 32 17 16 Fax: +32 (0)16 32 19 86
E-mail: jeroen.decoster@esat.kuleuven.ac.be

[*]IMEC, Kapeldreef 75, B-3001 Leuven, Belgium

Abstract— **This paper analyses the mechanical behaviour of various suspensions of electrostatically actuated RF MEMS switches. A family of capacitive switches is described, with suspensions varying step by step from cantilevers to meander shaped double clamped beams. The result is a capacitive shunt switch with a designed actuation voltage of 4.5 V, and 20dB isolation and 0.04 dB insertion loss at a frequency of 2 GHz. At the time of writing, the proposed devices are being processed.**

Keywords— RF MEMS; capacitive micromachined switch; electrostatic actuators; micromechanical devices

I. Introduction

A. Motivation

In the last decade, the large potential of MEMS devices in RF circuits has been demonstrated abundantly [1]. A lot of research effort has been put into electrostatically actuated RF switches. However, the integration of these devices into RF front-ends is being hampered partly as a result of the high pull-in voltage (15 – 50 V) in [2-5]. Nevertheless, low actuation voltages can be achieved and have been demonstrated by [3,8,9]. The main issue in this respect is to make a good compromise between low actuation voltage and other requirements, such as RF performance, shock and vibration resistance. The switches presented here have designed actuation voltages as low as 4.5 V. This makes them suitable for use in battery-operated systems. A schematic cross-section is shown in Figure 1.

B. Aim of the design

The following well-known formula gives the actuation voltage of any electrostatically operated member,

$$V_{pi} = \sqrt{\frac{8k_z g^3}{27A\varepsilon_0}}, \quad (1)$$

where k_z is the mechanical stiffness of the underetched structure, g is the zero-voltage gap spacing between top and bottom electrode of the actuator and A is the surface area of the actuator. From this formula, it can be found that the only means for lowering the actuation voltage are an increase in the area A or a decrease in the mechanical stiffness of the suspension, k. The gap-spacing g was not considered to be an adjustable parameter, as the design was done within the framework of the PASSI™ process [7]; the gap-spacing used in this process is optimised for good RF performance. Since A is directly related to the isolation and insertion loss, the surface can not be made arbitrarily high. As a result, low pull-in voltages are obtained when designing in the first place for a low mechanical stiffness [8], yet high mechanical resonance frequency.

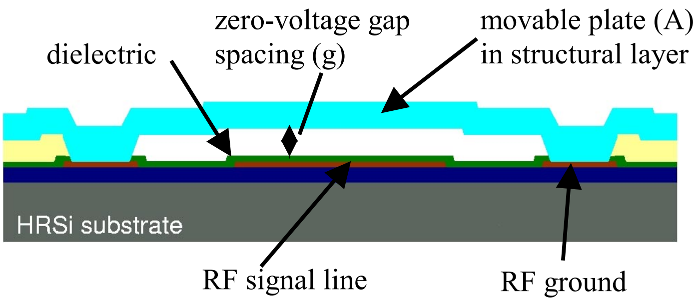

Figure 1 Cross-section of capacitive shunt switch.

TABLE 1 GEOMETRY OF SHUNT SWITCHES.

L_c	475 µm	length of coupling area
b_c	275 µm	width of coupling area
L_b	200 µm	length of beam segments
w	20 µm	width of beams
t	5 µm	thickness of structural layer
g	3 µm air & 0.2 µm Si_xN_y	gap between top and bottom electrode

II. CAPACITIVE SHUNT SWITCHES

A. Structural design

Figure 2 shows a number of capacitive shunt switches, with suspensions varying from simple cantilever beams to meander shaped springs. When applying a DC bias

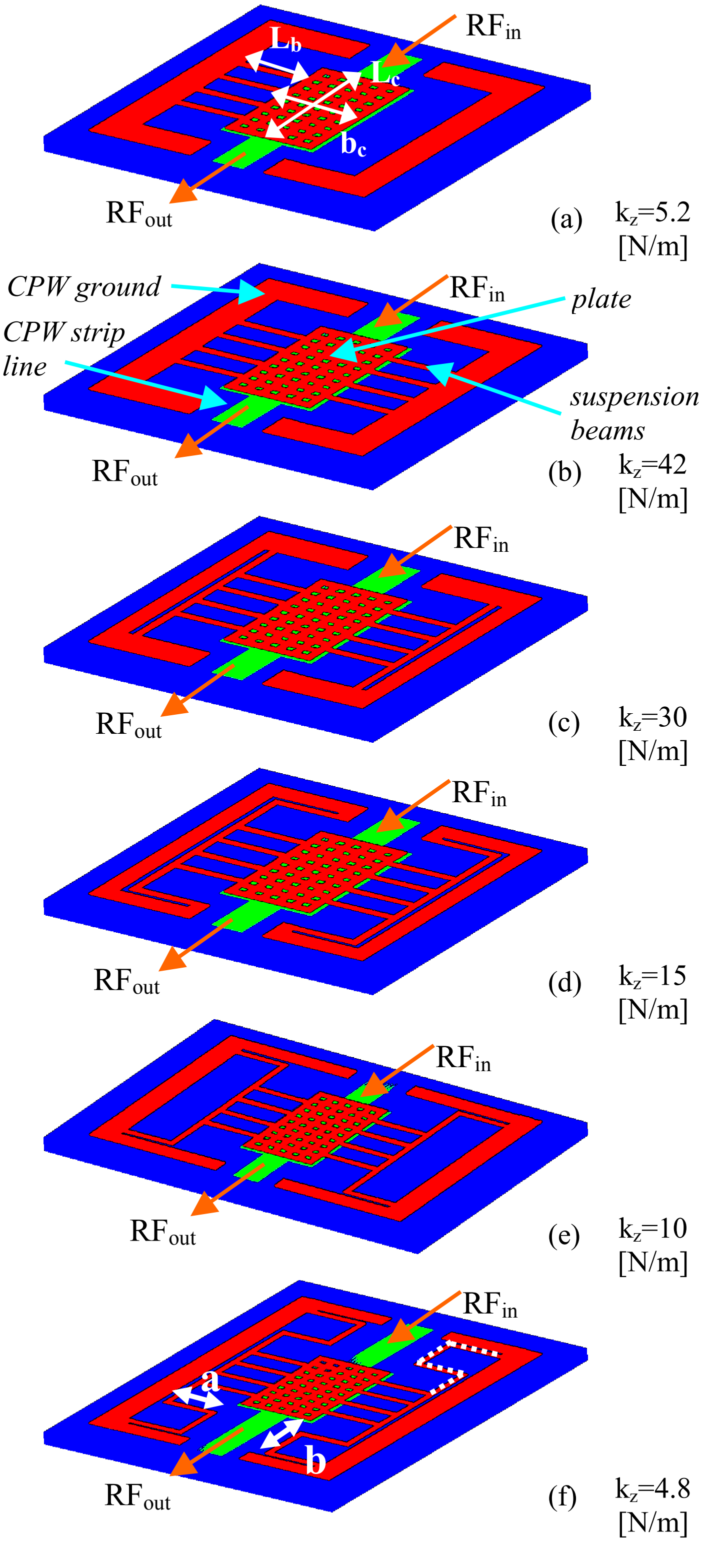

Figure 2. A family of capacitive shunt switches with various suspensions.

voltage between the coplanar waveguide (CPW) ground and the CPW stripline, the perforated plate is attracted towards the substrate, thus lowering the shunt impedance to ground and reflecting the incident wave. The basic dimensions of these switches are given in Table 1 (values given in this table are applicable to all devices studied).

The cantilever structure shown in Figure 2a is the most straightforward approach to obtain a low mechanical stiffness and actuation voltage. However, this device is very susceptible to sticking as well as warpage after releasing due to internal stress gradients in the aluminium structural layer. This may result in a large discrepancy between designed and measured values of the actuation voltage [9]. Apart from exhibiting a low stiffness, the suspension should therefore also prevent the switch from deforming excessively. This can be achieved by altering the geometry of the suspension [10]. Accordingly, the devices in Figure 2b-f are suspended symmetrically. It is expected this will result in a smaller and more uniform deformation. In each step from Figure 2b to f, a number of beam segments with length L_b is added until the stiffness approaches the same value as for the cantilever switch in Figure 2a.

The mechanical deformation of the switches in the actuated state was calculated both analytically and using the commercially available finite element software package CoventorWare^{TM} [11]. Figure 3 shows the displacement of the switch from Figure 2f as a function of the applied bias voltage. The difference between the pull-in and release voltage is obvious. As an example, Table 2 compares the results obtained by the finite element method (FEM) and analytic solutions for a meander as indicated by the dotted line in Figure 2f. The analytic expression which was used in the table can be found by imposing a shear force and a torsion moment as well as a bending moment to keep the cross-section at the end of the meander horizontal in the x- and y-directions:

$$\frac{1}{k_z}=\frac{8b^3}{3EI}+\frac{a^3}{6EI}+\frac{a^2b}{2Gk_T}+\frac{5ab^2}{Gk_T}-\frac{\left(2b^2/EI+3ab/Gk_T\right)^2}{2a/Gk_T+2b/EI}, \tag{2}$$

where a and b are the dimensions of the beam segments as indicated in Figure 2f, E is the Young's modulus of the material in the structural layer, G is the shear modulus, and k_T is a torsion characteristic for the cross-section of the beams as found in [12]:

$$k_T=wt^3\left(\frac{1}{3}-0.21\frac{t}{w}\left(1-\frac{t^4}{12w^4}\right)\right), \tag{3}$$

where w is the with of the suspension beams and t is the thickness of the structural layer.

The area moment of inertia of the beam cross section, I, is given by:

$$I=\frac{wt^3}{12}. \tag{4}$$

TABLE 2 MECHANICAL STIFFNESS OF MEANDER [N/m].

DIMENSION [µm]	FEM	ANALYTIC, (2)	REL. DIFF. [%]
a=180,b=60	6.70	6.66	-0.6
a=130,b=60	12.5	12.7	+1.6
a=280,b=60	2.46	2.39	-2.8
a=180,b=45	8.38	8.24	-1.7
a=180,b=90	4.29	4.33	+0.9
a = b = L_b	2.31	2.37	+2.6

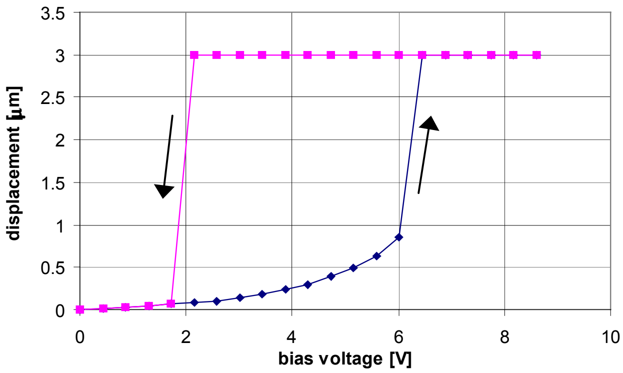

Figure 3. Simulated hysteresis of an electrostatically actuated switch.

B. Summary: expected performance

Apart from the pull-in voltage, there are several other very important aspects, which were evaluated for the components shown in Figure 2.

Concerning the reliability of the devices, no standard exists at present which specifies e.g. the minimum required resonance frequency. One can only ensure that the resonance frequency is kept above an arbitary value. In the studied devices, resonance was therefore verified to occur at higher frequencies than 10 kHz wherever possible.

Another measure for device reliability is the shock-survivability. It has been verified whether the stresses in the structural layer do not exceed a safety margin when the device is subjected to an accleration of 1000g. The safety limit was set at 5% of the fracture strength of the material (aluminium in this case). Accordingly, the maximum Mises stress in the structural layer was limited to 30 MPa when an acceleration in the Z-direction of 1000g is applied externally. For the stiffest devices, the deflection is only 0.1 µm under such acceleration, but the most compliant device has a deflection in the order of 1 µm in this case. The devices with the highest compliancy are therefore only suitable for applications where the external accelerations are limited.

As to the RF properties, the insertion loss and the isolation were determined analytically at a center frequency of 2GHz. Table 3 summarises all of the above.

TABLE 3 GENERAL PROPERTIES OF CAPACITIVE SWITCHES.

#	V_{pi} [V]	f_{res} [kHz]	σ_{max} @ 1000g	Insertion loss [dB]	Isolation [dB]
a	6.4	9.2	4.5 MPa	0.04	20
b	18	25	2.3 MPa	0.04	20
c	15	19	8.5 MPa	0.04	20
d	11	13	15 MPa	0.04	20
e	8.9	11	13 MPa	0.04	20
f	6.2	6.9	17 MPa	0.04	20
f'	4.5	5.0	24 MPa	0.04	20

f': modified version of f, where L_b=300

III. MODIFIED CAPACITIVE SHUNT SWITCHES

In spite of the symmetry in the suspensions shown, they are still prone to deformation due to residual stresses and stress gradients in the structural layer. Therefore, two modified designs were studied, which are entirely insusceptible to deformation in case of tensile residual stresses. The layouts of these devices are shown in Figure 4.

The switch in Figure 4a is suspended in a fixed frame, and since this suspension has identical stiffnesses in the x- and y-directions, no deformation will occur due to in-plane tensile stresses. The inner frame in Figure 4b results in a 10% increase of the z-axis compliancy of the device while consuming the same die-area and reducing the length of the beams between the joints.

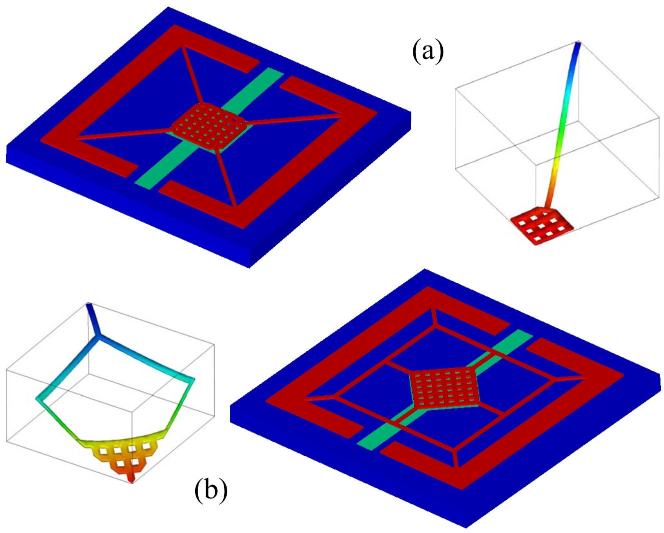

Figure 4. Modified designs of capacitive switch.

IV. CONCLUSIONS

A number of capacitive shunt switches was designed and the expected performance has been studied by analytical and numerical models. The devices are currently being processed in order to verify the proposed results. The main objective of this work was to realise RF MEMS components with low actuation voltage.

V. ACKNOWLEDGEMENTS

This work is supported by the European Commission, MEMS2TUNE project IST-2000-28231 within the IST Programme. The authors gratefully acknowledge the cooperation with all the partners involved in this project: Alcatel Space, Ericsson Radiosystems and Philips Electronics.

VI. REFERENCES

[1] H.A.C. Tilmans, MEMS components for wireless communications (invited paper), *Proceedings of EUROSENSORS XVI*, Prague, Czech Republic, 2002, pp. 1-34.

[2] J. B. Muldavin, and G. M. Rebeiz, High Isolation CPW MEMS Shunt Switches, Part 2: Design, *IEEE Transactions on Microwave Theory and Techniques*, 1999.

[3] Z. J. Yao, S. Chen, S. Eshelman, D. Denniston, and C. Goldsmith, Micromachined Low-Loss Microwave Switches, *IEEE Journal of Microelectromechanical Systems*, Vol. 8, No. 2, 1999.

[4] C. Wang, R. Ramadoss, S. Lee, K. C. Gupta, V. M. Bright, and Y. C. Lee, Flexible Circuit-Based RF MEMS Switches, *Proceedings of ASME International Mechanical Engineering* Congress and Exposition, New York, NY, 2001.

[5] S. Pacheco, C. T.-C. Nguyen, and L. P. B. Katehi, Micromechanical electrostatic K-band switches, *Proceedings of IEEE MTT-S International Microwave Symposium 1998*, pages 1569-1572, Baltimore, Maryland, 1998.

[6] D. Hah, E. Yoon and S. Hong, A low voltage actuated micromachined microwave switch using torsion springs and leverage, *Proceedings of IEEE MTT-S International Microwave Symposium*, Boston, MA, USA, 2000, pp. 1540-1543.

[7] J. van Beek et al, The integration of passives using thin-film technology on high-ohmic Si in combination with thick-film interconnect., *Proceedings of IMAPS International Symposium on Micro-Electronics*, Baltimore, MD, USA, 2001.

[8] D. Balaraman, S. K. Bhattacharya, F. Ayazi, and J. Papapolymerou, Low-Cost Low Actuation Voltage Copper RF MEMS Switches, *Proceedings of IEEE MTT-S International Microwave Symposium 2002*, Seattle, Washington, 2002.

[9] S. Pacheco, L. P. B. Katehi, and C. T.-C. Nguyen, Design of Low Actuation Voltage RF MEMS Switch, *Proceedings of IEEE MTT-S International Microwave Symposium 2000*, Boston, Massachusets, 2000.

[10] C.-F. Tsou, and W. Fang, The Effect of Residual Stress on Semicircular Microbeam, *Proceedings of ASME 1999 International Mechanical Engineering* Congress and Exposition, Nashville, Tennessee, 1999.

[11] http://www.coventor.com

[12] Roark, R., Young, W., Formulas for Stress and Strain, Mc Graw-Hill, New York, 1985.